24th COBEM - 2017

24th ABCM International Congress of Mechanical Engineering
December 3-8, 2017, Curitiba, PR, Brazil

COBEM-2017-0777
ANALYSIS OF RESTRICTIONS ON AN EXTENDED TIME DELAY FEEDBACK CONTROL APPLIED TO A SMA-PENDULUM SYSTEM

Dimitri Danulussi Alves Costa
Marcelo Amorim Savi
Center for Nonlinear Mechanics, COPPE - Department of Mechanical Engineering
Universidade Federal do Rio de Janeiro
21.941.972 – Rio de Janeiro – RJ, Brazil, P.O. Box 68.503
dimitri.d.costa@gmail.com, savi@mecanica.ufrj.br

Abstract. *This work deals with the extend time delay feedback control of an SMA-pendulum system. The SMA elements are used to control the system's dynamics been in two different ways: as ideal actuators and as constrained actuators. The energy equation is used to model the constrained actuator and the differences between the ideal control and constrained control are analyzed by the Floquet exponents of the stabilized UPO. The influence of the errors on the Floquet exponents themselves is performed by varying the convection coefficient on the SMA elements. Results show that the control of the period 1 and period 2 UPO are possible within a certain limit of restrictions.*

Keywords: *Nonlinear Dynamics, Chaos Control, Shape Memory Alloys.*

1. INTRODUCTION

Various non-linear system on engineering can be represented by a pendulum equation like electrical motors (Chen et al., 2014), torsional dampers (Monroe and Shaw, 2013), ankles (Suzuki *et al.*, 2012) and cranes (Ju *et al.*, 2006). A typical example of this systems is discussed by De Paula *et al.* (2006), where an experimental-numerical investigation is performed. Results show several complex responses that include bifurcations, chaos and transient chaos. Also, the study of nonlinear control on these systems are reported in several works (Bessa *et al.*, 2009; de Paula and Savi, 2009; Pan *et al.*, 2013).

The pioneering work of Pyragas (1992) proposed the first chaos control technique letter extended by Socolar *et al.* (1994). These approaches are based on a time delayed feedback (TDF) of the output signal and take advantage of the embedded unstable periodic orbits on a chaotic attractor to reduce the control energy cost. This controller and its variations are applied in various electrical systems on the literature, but only a few works focus on mechanical applications and the robustness to actuation modeling or actuation errors of these controller (Bessa *et al.*, 2009; de Paula and Savi, 2009, 2011; de Souza and Caldas, 2004a; Leiva and Briozzo, 2006). The use of this kind of control can be exploited in different mechanical systems including non-smooth systems (Battelli and Feckan, 2013; de Souza and Caldas, 2004b; Savi *et al.*, 2007), smart material systems (Savi, 2015), machining (Litak *et al.*, 2009a, 2009b), energy harvesting (Barbosa *et al.*, 2015), among others.

Shape memory alloys (SMAs) are known by their adaptability due to the thermomechanical coupling of their properties. This coupling is due to phase transformations on the material that imply the effects of shape memory and pseudoelasticity. The first is the ability to completely recover a residual strain by a proper thermomechanical loading process. The other is a complete strain recovery of the material with a large hysteresis in a loading-unloading cycle. These materials are already studied and used as actuators in a variety of studies (Bertolino et al., 2017; Bhattacharyya et al., 1995; Jayender et al., 2008; Kim et al., 2006), but none of them performs a deep analysis of the SMA thermal restrictions and the actuation frequency. Other uses of SMA can be found on vibration control (Bessa et al., 2013), origami structures (Kuribayashi et al., 2006), robotics (Kim et al., 2006) and energy harvesting (Lebedev et al., 2011), showing a broad use and potential for a variety of applications.

This work tries to combine chaos control and the adaptive behaviour of SMA's by investigating the nonlinear dynamics of an SMA-Pendulum system composed of a nonlinear pendulum coupled with SMA springs. The system presents a variety of responses ranging from periodic to chaotic depending on the temperature applied to the SMA springs. Dynamical analysis of the chaotic response is carried out and the extended time delay feedback method

(Socolar et al., 1994) is applied by a restricted SMA actuator. This restriction introduces errors on the actuation force which raises the Floquet exponents of the controlled UPO. Comparisons between the constrained actuator and an ideal one, and also, between the restrictions time scale and the UPO's frequency are performed.

2. PENDULUM SYSTEM

The pendulum system (Fig. 1) is formed by a disc of diameter D(1), and a lumped mass m (2). The excitation is provided by a DC motor (7) with an arm length b, connected to a string-spring system. The springs are made of SMA providing an adaptive behavior to the system. The two SMA springs (6) are connected by a string which is wrapped on a disc of diameter d (pendulum coupling). In one end the first string is connected to the DC motor. The second spring is connected to an anchor (5). A magnetic device provides a controlled dissipation to the apparatus (3). A similar system is presented by De Paula e al. (2006).

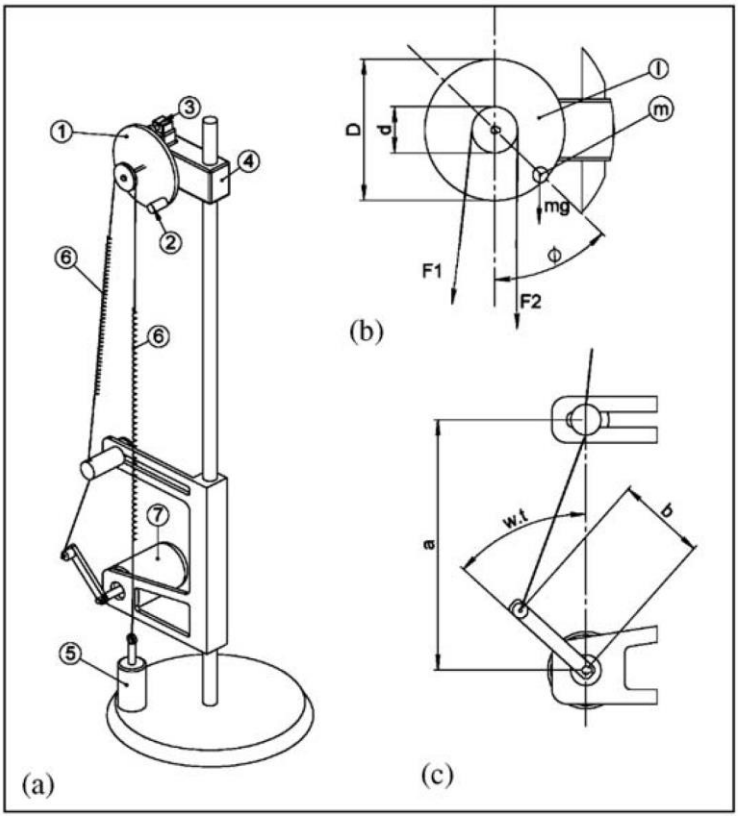

Figure 1. Nonlinear pendulum: a) physical model (1) metallic disc; (2) lumped mass; (3) magnetic damping device; (4) rotary motion sensor; (5) anchor or mechanical arm; (6) SMA springs; (7) electric motor; b) Parameters and forces on the metallic disc; c) Parameters for driving device (de Paula et al., 2006).

By considering that ϕ is the angle of the pendulum and assuming that the dissipation is a combination of linear viscous and dry friction, the equation of motion is given by:

$$\phi'' = -\frac{\vartheta}{J\omega_0}\phi' - \frac{\xi}{mgD}sign(\phi') - \frac{sin(\phi)}{2} + \frac{d}{2mgD}(F_m - s_m) \tag{1}$$

where J is the angular inertia of the pendulum, g is the acceleration of gravity, ϑ is the viscous dissipation coefficient, ξ is the dry friction coefficient and ω_0 is a reference frequency defined as follows,

$$\omega_0 = \sqrt{\frac{mgd}{I}} \tag{2}$$

Time derivative $(\,)'$ is related to a dimensionless time defined by $t^* = t\omega_0$. Moreover, s_m is the force of the anchored spring and F_m is the excitation force of the motor-string-spring system.

The displacement (u) due to the movement of the motor can be given as:

$$u = \sqrt{\left(a^2 + b^2 - 2 \cdot \left[abcos\left(\frac{\omega t^*}{\omega_0} + \theta\right)\right]\right)} - (a - b) - \frac{d\phi}{2} \tag{3}$$

where a is the distance between the center of the disc and the center of the rotor, θ is the initial phase of the motor, ω is the excitation frequency and b is the motor arm length.

Different models are proposed to describe the thermomechanical behavior of SMAs (Lagoudas, 2008; Paiva et al., 2005), and specifically for springs (Aguiar et al., 2010; Enemark et al., 2016). For the sake of simplicity, a polynomial model is employed following the stress-strain (σ-ε) relation given by,

$$\sigma = a_m^*(T - T_M)\varepsilon - b_m^*\varepsilon^3 + \frac{{b_m^*}^2}{a_m^*(T_A - T_M)}\varepsilon^5 \tag{4}$$

where a_m^* and b_m^* are material parameters, T_M is the temperature below which only martensitic phase is stable, T_A is the temperature above which only austenitic phase is stable (at stress-free scenario), T is the temperature of the SMA. Based on that, and assuming that phase transformation is homogeneous for the spring cross-section, it is possible to write a force-displacement equation for each spring that is formally similar to this stress-strain expression (Aguiar et al., 2010). Hence, for spring 1:

$$F_m = a_m(T_1 - T_M)u - b_m u^3 + \frac{{b_m}^2}{a_m(T_A - T_M)}u^5 \tag{5}$$

where T_1 is the temperature on spring 1. And for spring 2, where T_2 is the temperature on the spring:

$$s_m(T_2, \phi) = a_m(T_2 - T_m)\frac{\phi d}{2} - b_m\left(\frac{\phi d}{2}\right)^3 + \frac{{b_m}^2}{a_m(T_A - T_m)}\left(\frac{\phi d}{2}\right)^5 \tag{6}$$

We consider that the temperature of the SMA can be altered by a current I_1 on the SMA springs trough Joule effect. Two possible controllers are considered. The first one is an ideal controller with no thermal restrictions which can provide any actuation force at any time. The second is a constrained controller where the current I_1 is restrained to a certain limit and the temperature T_1 at the SMA is given by the energy equation.

By considering that the ambient functions as a thermal bath, that the SMA spring has a constant resistance, is homogeneous in its properties and temperature, and that all the heat is produced by the Joule effect the energy equation for the SMA springs is given by:

$$\dot{T}_1 = -\frac{h}{c_p}(T_1 - T_\infty) + \frac{\left(I_1 + I_{ref}\right)^2 R_{ohn}}{c_p} \tag{7}$$

where T_∞ is the ambient temperature, I_1 is the current on the spring, I_{ref} is a reference current which maintains the system on the reference temperature T_{ref}, R_{ohn} is the spring resistance, c_p is the spring thermal capacity and h is the convection dissipation coefficient. It is important to notice that Eq. 7 restricts the accessible temperatures and actuation forces, also the factor $\frac{h}{c_p}$ dictates the time scale of the cooling process restricting the actuation frequency.

The actuation force is given by:

$$F_{thermo} = a_m\left[\left(T_1 - T_{ref}\right)u\right] \tag{8}$$

The actuation force is introduced on the system as:

$$\phi'' = f(\phi, \phi', t^*, ref) + \frac{1}{mgD}F_{thermo}(T_1) \tag{9}$$

The difference between the calculated control force and the applied forces by the constrained controller can be defined as an error percentage of the maximum applied force (e_T), being expressed as:

$$e_T = \frac{F_{thermo}(l, T_1) - z(y,t)}{max\big(z(y,t)\big)} \tag{10}$$

Where z is the actuation force and y the observable variable. The energy consumption of the actuation is given by:

$$E_T = \int_0^t I_1^2 R_{ohn} dt' \tag{11}$$

3. ETDF CONTROL

The goal of a chaos control method is to stabilize an unstable periodic orbit (OPI) that is embedded on a chaotic attractor. To do so the extended time delay feedback control uses the sum of delayed observables which can be expressed as:

$$\begin{cases} \dot{x} = f(x,t) + z(y, y(t-\tau), y(t-2\tau), \dots) \\ y(t) = C(x)x \\ z(y,t) = K\left[(1-r)\sum_{n=1}^{\infty} r^{n-1} y(t-n\tau) - y(t)\right] \end{cases} \tag{12}$$

where $x \in \mathbb{R}^m$ is the system state, $f(x,t) \in \mathbb{R}^m$ defines the system dynamics and t is the time; $z \in \mathbb{R}^m$ is the control signal; $y \in \mathbb{R}^n$ is the system observation provided by the operator $C(x) \in \mathbb{R}^n \otimes \mathbb{R}^m$ applied to state variables; $K \in \mathbb{R}^m \otimes \mathbb{R}^n$ is an proportional gain and $r \in \mathbb{R}$ a controller parameter, τ is the period of the target UPO to be controlled. Control parameters K and r can be estimated by various methods including the calculation of the UPO's Lyapunov exponents (de Paula et al., 2014; de Paula and Savi, 2009; Pyragas and Tamaševičius, 1993) or Floquet theory (Just et al., 1997; Pyragas, 2006).

On this work the Floquet approach will be applied as Floquet exponents (μ) calculation requires only one time period of integration. Also the parameter K is considered to be a scalar resulting in $c(x) \in \mathbb{R}^m$ and $z \in \mathbb{R}$. After their determination the stability of the UPO can be analyzed as follows: if all exponents have a negative real part, the orbit is stable, while if any Floquet exponent has a positive real part, the orbit is unstable.

To calculated the Floquet exponents one may follow the procedure used by Pyragas (2006). One first perform a linearization on the vicinities of the UPO's path $x_0(t)$ by assuming a displacement from the UPO of the form:

$$\delta x = x(t) - x_0(t) \tag{13}$$

With a time evolution given by:

$$\delta\dot{x} = Df(t, x_0) + KB\left[(1-r)\sum_{n=1}^{\infty} r^{n-1}\delta x(t-n\tau) - \delta x(t)\right] \tag{14}$$

where Df is the Jacobian matrix, B is the gradient of the function c with respect to its variables.

So to apply the Floquet theory it is assumed that the displacements from the UPO have an exponential envelope given by:

$$\delta x(t-n\tau) = e^{-\mu n\tau}\delta x(t) \tag{15}$$

Considering that the observable variable y depends of only one state of the system x_j. This leads to:

$$\delta\dot{x} = \left(Df(t, x_0) + K\frac{1 - e^{-\mu_j\tau}}{1 + re^{-\mu_j\tau}}B\right)\delta x \tag{16}$$

Equation 15 correlates all de delayed states which reduces the dimension of equation 16 to just the dimension of δx. The tradeoff here is that now Eq. 16 depends on the Floquet exponents themselves. Finally one can compute the fundamental matrix ψ at time τ by integrating its time evolution equation given by:

$$\psi' = \left(Df(t, x_0) + K \frac{1 - e^{-\mu_j \tau}}{1 + re^{-\mu_j \tau}} B \right) \psi$$
$$\psi(0) = \mathbb{I} \tag{17}$$

And obtain the Floquet exponents by solving the following equation:

$$\psi(\tau, x_0, \mu) - e^{\mu \tau} \mathbb{I} = 0 \tag{18}$$

Since matrix $\psi(\tau, x_0, \mu)$ depends on the Floquet exponents themselves, it is necessary to perform an optimization procedure for their calculation. This procedure is based on a differential evolution algorithm (Storn and Price, 1997) and is presented in Fig. 2. Initially a first guess population of possible Floquet exponents is randomly generated (μ_0), afterwards the time integration of the fundamental matrix ψ is performed using Eq. 17, a fourth-order runge-kutta method and the first guess Floquet exponents. Afterwards a new set of exponents are calculated from $\psi(\tau, x_0, \mu_0)$ and compared with the first guess population. If the exponents do not satisfy the stop criterion the algorithm in (Storn and Price, 1997) is used to select the individuals of the population and create a new generation μ_{n+1} which becomes the new first guess. This process is repeated until the stopping criterion is achieved.

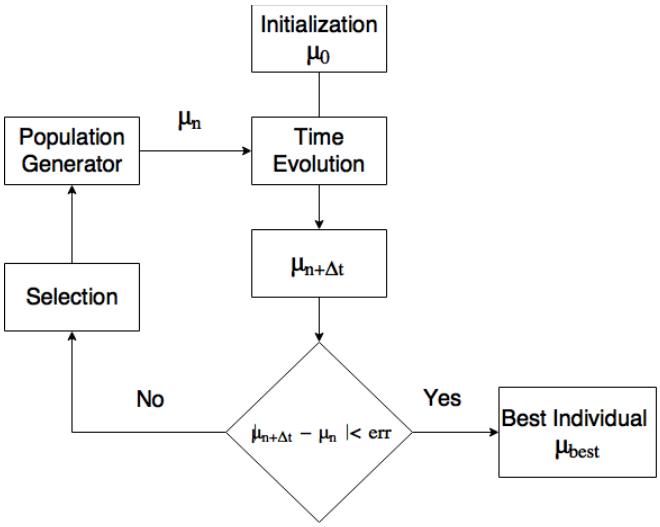

Figure 2. Algorithm to calculate the Floquet exponents with ETDF control. μ_0 is the initial guess for the Floquet exponent, μ_n indicates the nth population, $\mu_{n+\Delta t}$ is the calculated Floquet exponent population after time integration, **err** is the error tolerance, and μ_{best} is the best individual on the selected population.

4. NUMERICAL RESULTS

Numerical simulations are carried out by a Fourth-order Runge-Kutta method with the parameters presented in (de Paula et al., 2006): $m = 1.47\ kg$, $D = 9.5\ cm$, $d = 4.8\ cm$, $b = 1.5\ cm$, $a = 16\ cm$, $\xi = 1.272\ 10^{-4}\ Nm$, $\vartheta = 2.368\ \frac{kgm^2}{s}$, $g = 9.81\ m/s^2$. SMA parameters are adjusted with experimental data: $T_A = 289.35\ K$, $T_M = 282.45\ K$, $a_m = 0.4375\ N/mK$ and $b_m = 150\ Pa/m$. The thermal parameters are: $T_{ref} = 283.15\ K$, $h = 2\ W/K$, $c_p = 5\ J/K$ *and* $T_\infty = 281.15\ K$. It is important to highlight that all parameters used on this work can be related to real values on an experiment and can be used as bases to the construction of a physical apparatus. Time steps are chosen in such a way that errors are less than 10^{-8} estimated by a fifth-order method.

For a forcing frequency $\omega = 8.5\ \mathrm{rad/s}$ and initial conditions of $x_0 = (-6\ rad, 0\ rad/s)$ the system presents a chaotic response (Fig. 3) indicated by a positive Lyapunov exponent $\lambda = 2.86 \pm 0.01\ bit/s$. All Lyapunov exponents are calculated using the algorithm proposed by Wolf et al. (Wolf et al., 1985) and Floquet exponents (μ) are calculated employing the procedure described at section 2 (Pyragas, 2006). The UPO's of the system are identified by the algorithm proposed by Auerbach et al. (1987) with parameters $r_1 = 0.04$ and of $r_2 = 0.15$ and are presented on Fig. 4.

To perform the control it is considered that the velocity of the pendulum is the observable variable and the force applied by the change in temperature by the SMA spring is the control signal. The control force infinite sum is assumed to be a rapid converging series and is calculated up to its 10th term. Simulations are performed after a time integration of 75 periods so all variables for the control signal calculation are known. The initial condition for all simulations is $x_0 = (-6\ rad, 0\ rad/s)$.

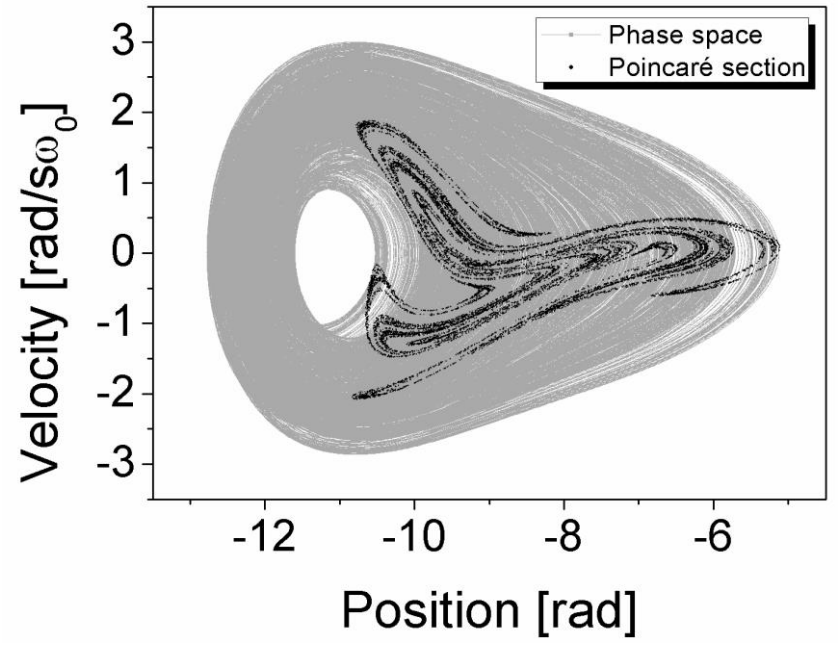

Figure 3. Phase space and Poincaré section of the chaotic response.

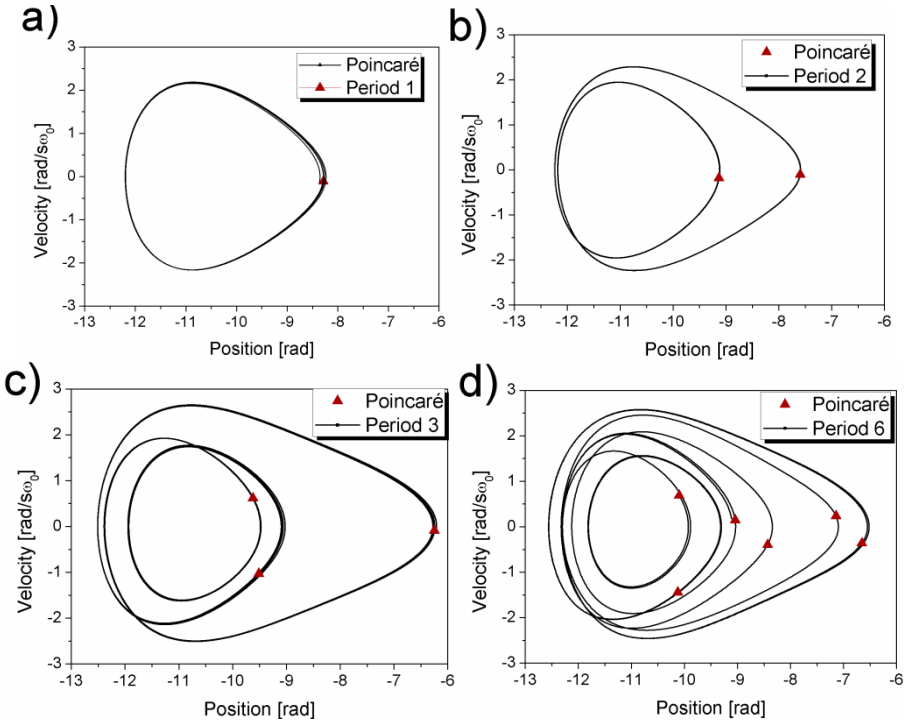

Figure 4. Phase space and Poincaré sections: a) period-1 UPO, b) period-2 UPO, c) period-3 UPO, d) period-6 UPO.

Initially the period 2 UPO is on focus. It is verified that for the ideal control and values of $r = 0.1$ and $K = 0.2$ the real part of the greater Floquet exponent is: $-0.19 \pm 0.03\ s^{-1}$. Figure 5 shows the ideal control with these parameters. The controller stabilizes the system in a time interval of 13 UPO's periods. For comparison the constrained controller with same parameters is displayed in Fig. 6. It shows that the power consumption after stabilization is about the same in both cases. This occurs because the control signal tends to vanish after the stabilization and, therefore, it is easier for the constrained actuator to generate the force needed. On Fig. 6e the time evolution of the error can be seen. It starts with values of about 30% while the actuation force required by the controller is high but it decreases together with the actuation force needed until it stabilizes at below 0.2 % of error. It also displays that the constrained controller stabilizes

the targeted UPO faster than the ideal one, in about 9 UPO's periods. This may be due to the system's dynamics itself, as when the actuation force is not been fully applied to the system it may push the response to a faster converging path embedded on the systems dynamics, while the ideal control exponentially approaches the targeted UPO. The Floquet exponents for the constrained actuation is $-0.18 \pm 0.03\ s^{-1}$, which is lower them the ideal one due to the actuation constrains.

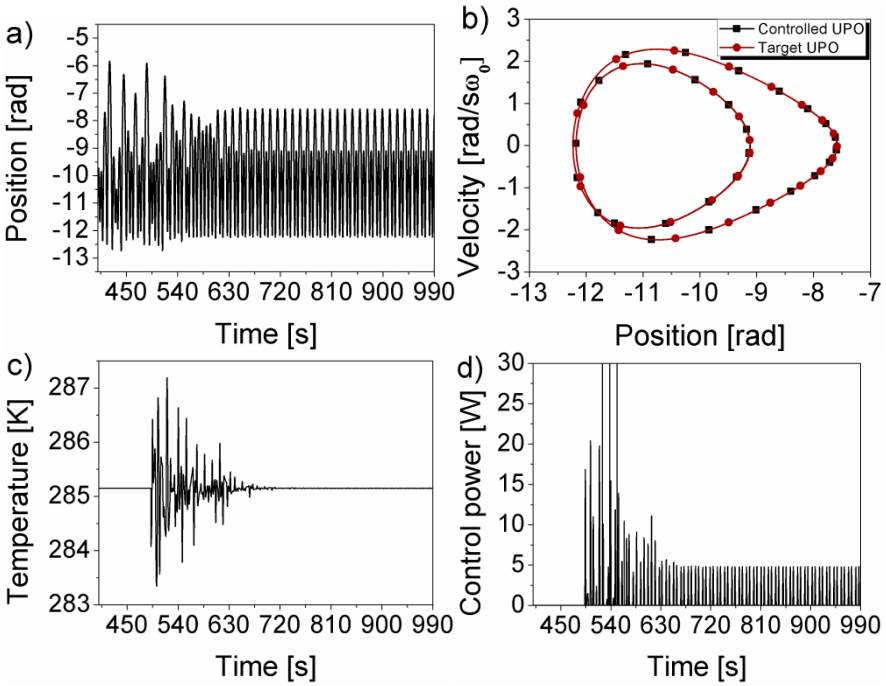

Figure 5: Standard ETDF control with ideal actuation of period-2 UPO. a) Pendulum position. b) Controller energy consumption. c) Stabilized orbit. d) Control Signal.

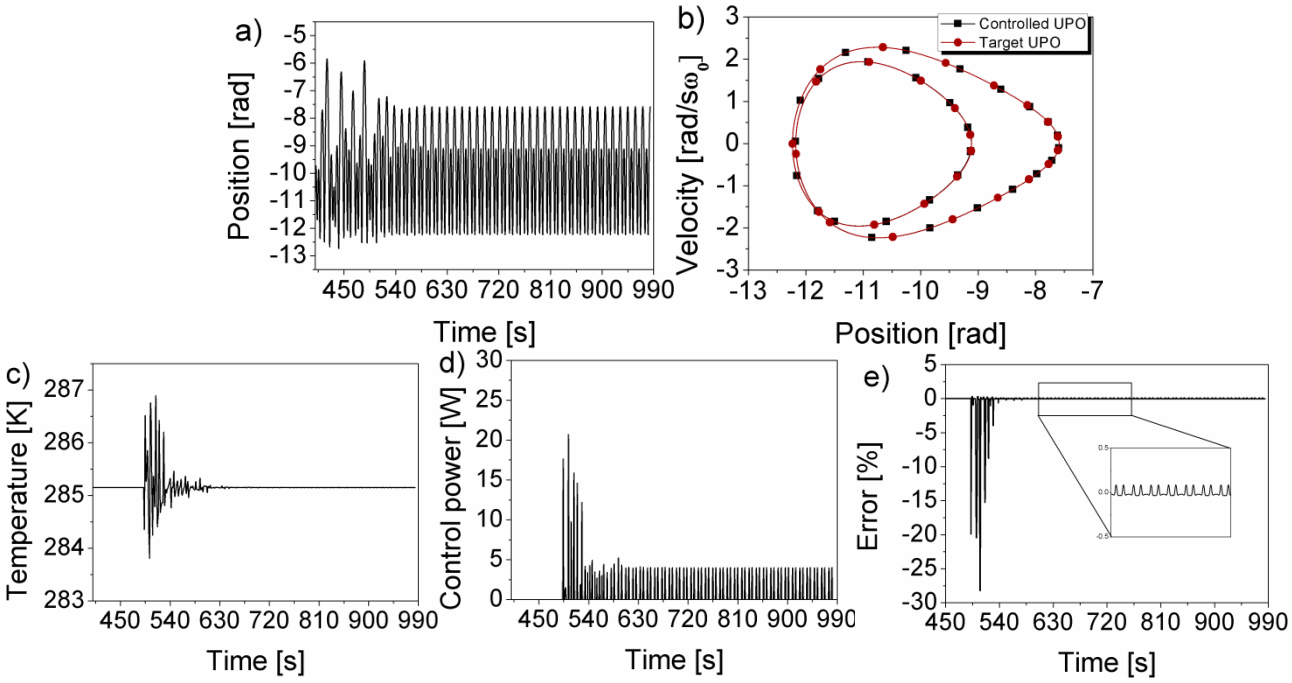

Figure 6: Constrained ETDF thermal control of period-2 UPO. a) Pendulum position. b) Controller energy consumption. c) Stabilized orbit. d) Control Signal. e) Actuation error, in detail the errors after stabilization.

To change the actuation errors amplitude and its influence on the system's response the parameter h can be varied. Figure 7 displays how the Floquet exponents change with the parameter h for the period-1 UPO with control parameters of $K = 0.4$ and $r = 0.3$. With high values of h the Floquet exponents approach their value with an ideal actuation (blue dotted line), while for lower values of h the Floquet exponents grow until their real part becomes positive implying that the UPO can not be stabilized by that set of parameters. Also it is important to notice that the Floquet exponents only raise significantly their value when the cooling rate, given by h/c_p, is lower them the targeted UPO frequency (vertical green dashed).

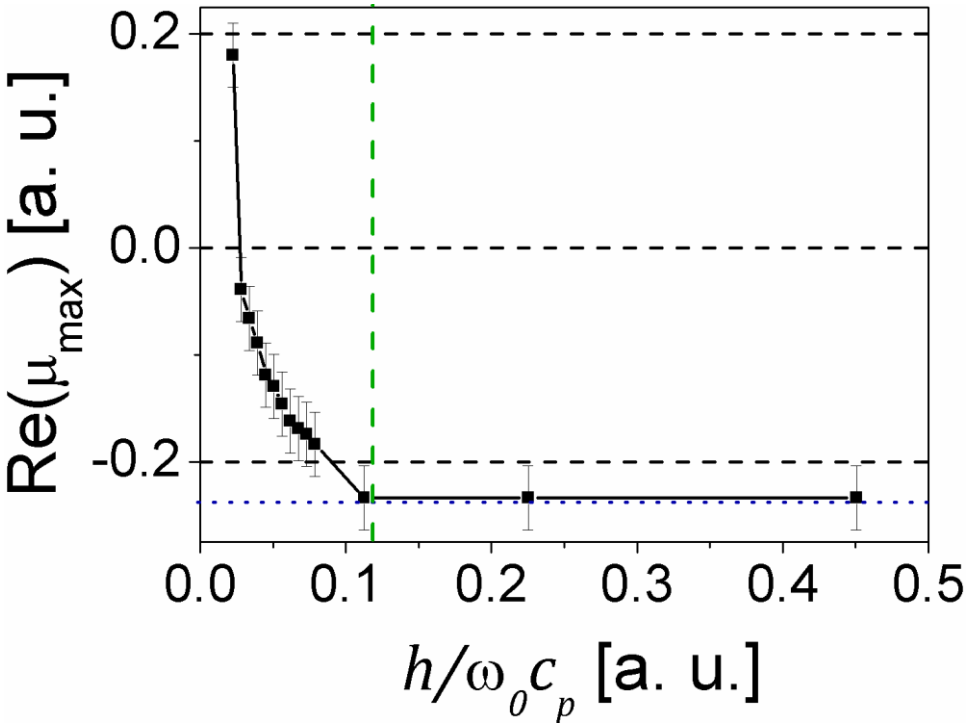

Figure 7: Floquet exponents against the cooling rate in non-dimensional units [a. u.] for the period-1 UPO constrained control. Blue dotted line: Floquet exponents with ideal control. Green dashed line: Frequency of period-1 UPO in a. u..

5. CONCLUSIONS

This work applies the extended time delay feedback control to stabilize unstable periodic orbits of an SMA-pendulum system. This control is provided by the SMA elements of the system in two different scenarios: one with an ideal actuation where it is assumed that all temperatures can be accessed by the SMA and another with a constrained thermal actuation with limits on the current applied and its time evolution dictated by the energy equation. One of the systems chaotic responses is characterized by its Lyapunov exponents and its UPOs are identified. The control parameters are set and its Floquet exponents are obtained to verify stabilization. Comparisons between the two scenarios are made showing that the ideal controller have lower Floquet exponents but can be slower to stabilize the UPOs due to the possibility of the second controller be helped by the systems dynamics. Results also show that after stabilization both controllers behave almost as equals as long as the Floquet exponents of the UPO are still negative. Analysis of the Floquet multipliers of the controlled UPOs shows that for low values of h the target UPO cannot be controlled due to the slow cooling rate of the actuator which lead to greater errors on the actuation signal. Besides, when convection tends to infinity, thermal controller tends to be similar to the ideal one.

This work opens the discussion about chaos control robustness against actuation errors and other types of uncertainties. It also opens the possibility of the application of SMA actuators on chaos control experiments as all parameters used on the simulations correspond to real experimental values.

6. ACKNOWLEDGEMENTS

The authors would like to acknowledge the support of the Brazilian Research Agencies CNPq, CAPES and FAPERJ. The Air Force Office of Scientific Research (AFOSR) is also acknowledged.

7. REFERENCES

Aguiar, R.A.A., Savi, M.A., Pacheco, P.M.C.L., 2010. Experimental and numerical investigations of shape memory alloy helical springs. Smart Materials and Structures 19, 025008. doi:10.1088/0964-1726/19/2/025008

Auerbach, D., Cvitanović, P., Eckmann, J.-P., Gunaratne, G., Procaccia, I., 1987. Exploring chaotic motion through periodic orbits. Physical Review Letters 58, 2387.

Barbosa, W.O.V., De Paula, A.S., Savi, M.A., Inman, D.J., 2015. Chaos control applied to piezoelectric vibration-based energy harvesting systems. The European Physical Journal Special Topics 224, 2787–2801. doi:10.1140/epjst/e2015-02589-1

Battelli, F., Feckan, M., 2013. Chaos in Forced Impact Systems. Discrete and Continuous Dynamical Systems- Series S 6, 861–890. doi:10.3934/dcdss.2013.6.861

Bertolino, G., Yawny, A., Pelegrina, J.L., 2017. The limitations of electrical resistance for accurate positioning of shape-memory actuators: The case of well-oriented CuZnAl single-crystals under uniaxial loading. Materials & Design 117, 316–325. doi:10.1016/j.matdes.2017.01.002

Bessa, W.M., de Paula, A.S., Savi, M.A., 2013. Adaptive fuzzy sliding mode control of smart structures. The European Physical Journal Special Topics 222, 1541–1551. doi:10.1140/epjst/e2013-01943-7

Bessa, W.M., de Paula, A.S., Savi, M.A., 2009. Chaos control using an adaptive fuzzy sliding mode controller with application to a nonlinear pendulum. Chaos, Solitons & Fractals 42, 784–791. doi:10.1016/j.chaos.2009.02.009

Bhattacharyya, A., Lagoudas, D.C., Wang, Y., Kinra, V.K., 1995. On the role of thermoelectric heat transfer in the design of SMA actuators: theoretical modeling and experiment. Smart Materials and Structures 4, 252.

Chen, L., Sun, X., Jiang, H., Xu, X., 2014. A High-Performance Control Method of Constant -Controlled Induction Motor Drives for Electric Vehicles. Mathematical Problems in Engineering 2014, 1–10. doi:10.1155/2014/386174

de Paula, A.S., dos Santos, M.V.S., Savi, M.A., Bessa, W.M., 2014. Controlling a Shape Memory Alloy Two-Bar Truss Using Delayed Feedback Method. International Journal of Structural Stability and Dynamics 14, 1440032. doi:10.1142/S021945541440032X

de Paula, A.S., Savi, M.A., 2011. Comparative analysis of chaos control methods: A mechanical system case study. International Journal of Non-Linear Mechanics 46, 1076–1089. doi:10.1016/j.ijnonlinmec.2011.04.031

de Paula, A.S., Savi, M.A., 2009. Controlling chaos in a nonlinear pendulum using an extended time-delayed feedback control method. Chaos, Solitons & Fractals 42, 2981–2988. doi:10.1016/j.chaos.2009.04.039

de Paula, A.S., Savi, M.A., Pereira-Pinto, F.H.I., 2006. Chaos and transient chaos in an experimental nonlinear pendulum. Journal of Sound and Vibration 294, 585–595. doi:10.1016/j.jsv.2005.11.015

de Souza, S.L.T., Caldas, I.L., 2004a. Controlling chaotic orbits in mechanical systems with impacts. Chaos, Solitons & Fractals 19, 171–178. doi:10.1016/S0960-0779(03)00129-2

de Souza, S.L.T., Caldas, I.L., 2004b. Calculation of Lyapunov exponents in systems with impacts. Chaos, Solitons & Fractals 19, 569–579. doi:10.1016/S0960-0779(03)00130-9

Enemark, S., Santos, I.F., Savi, M.A., 2016. Modelling, Characterisation and Uncertainties of Stabilised Pseudoelastic Shape Memory Alloy Helical Springs. Journal of Intelligent Material Systems and Structures.

Jayender, J., Patel, R.V., Nikumb, S., Ostojic, M., 2008. Modeling and Control of Shape Memory Alloy Actuators. IEEE Transactions on Control Systems Technology 16, 279–287. doi:10.1109/TCST.2007.903391

Ju, F., Choo, Y.S., Cui, F.S., 2006. Dynamic response of tower crane induced by the pendulum motion of the payload. International Journal of Solids and Structures 43, 376–389. doi:10.1016/j.ijsolstr.2005.03.078

Just, W., Bernard, T., Ostheimer, M., Reibold, E., Benner, H., 1997. Mechanism of time-delayed feedback control. Physical Review Letters 78, 203.

Kim, B., Lee, M.G., Lee, Y.P., Kim, Y., Lee, G., 2006. An earthworm-like micro robot using shape memory alloy actuator. Sensors and Actuators A: Physical 125, 429–437. doi:10.1016/j.sna.2005.05.004

Kuribayashi, K., Tsuchiya, K., You, Z., Tomus, D., Umemoto, M., Ito, T., Sasaki, M., 2006. Self-deployable origami stent grafts as a biomedical application of Ni-rich TiNi shape memory alloy foil. Materials Science and Engineering: A 419, 131–137. doi:10.1016/j.msea.2005.12.016

Lagoudas, D.C., 2008. Shape Memory Alloys, 1st ed. Springer US, Boston, MA.

Lebedev, G.A., Gusarov, B.V., Viala, B., Delamare, J., Cugat, O., Lafont, T., Zakharov, D.I., 2011. Thermal energy harvesting using shape memory/piezoelectric composites, in: Solid-State Sensors, Actuators and Microsystems Conference (TRANSDUCERS), 2011 16th International. IEEE, pp. 669–670.

Leiva, A.M., Briozzo, C.B., 2006. Control of chaos and fast periodic transfer orbits in the Earth–Moon CR3BP. Acta Astronautica 58, 379–386. doi:10.1016/j.actaastro.2005.12.006

Litak, G., Sen, A.K., Syta, A., 2009a. Intermittent and chaotic vibrations in a regenerative cutting process. Chaos, Solitons & Fractals 41, 2115–2122. doi:10.1016/j.chaos.2008.08.018

Litak, G., Syta, A., Wiercigroch, M., 2009b. Identification of chaos in a cutting process by the 0–1 test. Chaos, Solitons & Fractals 40, 2095–2101. doi:10.1016/j.chaos.2007.09.093

Monroe, R.J., Shaw, S.W., 2013. Nonlinear Transient Dynamics of Pendulum Torsional Vibration Absorbers—Part I: Theory. Jounrla of VIbration and Acoustics 135. doi:10:1115/1.4007561

Paiva, A., Savi, M.A., Braga, A.M.B., Pacheco, P.M.C.L., 2005. A constitutive model for shape memory alloys considering tensile–compressive asymmetry and plasticity. International Journal of Solids and Structures 42, 3439–3457. doi:10.1016/j.ijsolstr.2004.11.006

Pan, Y., Zhou, Y., Sun, T., Er, M.J., 2013. Composite adaptive fuzzy H∞ tracking control of uncertain nonlinear systems. Neurocomputing 99, 15–24. doi:10.1016/j.neucom.2012.05.011

Pyragas, K., 2006. Delayed Feedback Control of Chaos. Phylosophical Transactions of the Royal Society 364, 2309–2334.

Pyragas, K., 1992. Continuous Control of Chaos by Self-Controlling Feedback. Physics Letters A 170, 421–428.

Pyragas, K., Tamaševičius, A., 1993. Experimental control of chaos by delayed self-controlling feedback. Physics Letters A 180, 99–102.

Savi, M.A., 2015. Nonlinear dynamics and chaos in shape memory alloy systems. International Journal of Non-Linear Mechanics 70, 2–19. doi:10.1016/j.ijnonlinmec.2014.06.001

Savi, M.A., Divenyi, S., Franca, L.F.P., Weber, H.I., 2007. Numerical and experimental investigations of the nonlinear dynamics and chaos in non-smooth systems. Journal of Sound and Vibration 301, 59–73. doi:10.1016/j.jsv.2006.09.014

Socolar, J.E.S., Sukow, D.W., Gauthier, D.J., 1994. Stabilizing unstable periodic orbits in fast dynamical systems. Physical Review E 50, 3245–3248.

Storn, R., Price, K., 1997. Differential evolution–a simple and efficient heuristic for global optimization over continuous spaces. Journal of global optimization 11, 341–359.

Suzuki, Y., Nomura, T., Casadio, M., Morasso, P., 2012. Intermittent control with ankle, hip, and mixed strategies during quiet standing: A theoretical proposal based on a double inverted pendulum model. Journal of Theoretical Biology 310, 55–79. doi:10.1016/j.jtbi.2012.06.019

Wolf, A., Swift, J.B., Swinney, H.L., Vastano, J.A., 1985. Determining Lyapunov Exponents From a Time Series. Physica D 16, 285–317.

8. RESPONSIBILITY NOTICE

The authors are the only responsible for the printed material included in this paper.